Published in final edited form as:

J Comp Neurol. 2018 June 01; 526(8): 1389–1402. doi:10.1002/cne.24415.

Efferent projections of excitatory and inhibitory preBötzinger Complex neurons

Cindy F. Yang and **Jack L. Feldman***

Department of Neurobiology, David Geffen School of Medicine, UCLA, Los Angeles, California 90095-1763

Abstract

The preBötzinger Complex (preBötC), a compact medullary region essential for generating normal breathing rhythm and pattern, is the kernel of the breathing central pattern generator (CPG). Excitatory preBötC neurons in rats project to major breathing-related brainstem regions. Here, we provide a brainstem connectivity map in mice for both excitatory and inhibitory preBötC neurons. Using a genetic strategy to label preBötC neurons, we confirmed extensive projections of preBötC excitatory neurons within the brainstem breathing CPG including the contralateral preBötC, Bötzinger Complex (BötC), ventral respiratory group (VRG), nucleus of the solitary tract (NTS), parahypoglossal nucleus, parafacial region (RTN/pFRG or alternatively, pF_L/pF_V), parabrachial and Kölliker-Füse nuclei, as well as major projections to the midbrain periaqueductal gray (PAG). Interestingly, preBötC inhibitory projections paralleled the excitatory projections. Moreover, we examined overlapping projections in the pons in detail and found that they targeted the same neurons. We further explored the direct anatomical link between the preBötC and suprapontine brain regions that may govern emotion and other complex behaviors that can affect or be affected by breathing. Forebrain efferent projections were sparse and restricted to specific nuclei within the thalamus and hypothalamus, with processes rarely observed in cortex, basal ganglia, or other limbic regions, e.g., amygdala or hippocampus. We conclude that the preBötC sends direct, presumably inspiratory-modulated, excitatory and inhibitory projections in parallel to distinct targets throughout the brain that generate and modulate breathing pattern and/or coordinate breathing with other behaviors, physiology, cognition, or emotional state.

Graphical abstract

*Address for correspondence: Jack L. Feldman, Box 951763, Department of Neurobiology, David Geffen School of Medicine, UCLA, Los Angeles, California 90095-1763, Tel: 310-825-1586, feldman@g.ucla.edu.

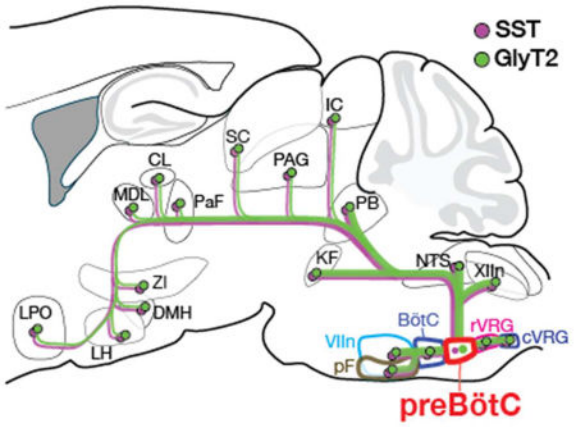

The preBötzinger Complex (preBötC) in the brainstem generates inspiratory rhythm, but how it is wired within the core central pattern generator neural circuit to produce and modulate breathing movements remains to be determined. We examined the connectivity of two populations of preBötC neurons, one excitatory expressing the peptide somatostatin (SST) and one inhibitory expressing the glycine transporter GlyT2, to other brainstem regions that modulate breathing and identified projections to suprapontine regions that may regulate voluntary and emotional control of breathing. PreBötC inhibitory projections parallel excitatory projections and, at least in the pons, may target the same neurons. Our brain-wide connectivity mapping shows that the preBötC sends direct, presumably inspiratory-modulated, excitatory and inhibitory projections in parallel to distinct targets throughout the brain.

Keywords

preBötzinger Complex; breathing; neural circuit; respiration; RRID: IMSR_JAX:013044; RRID: IMSR_RBRC04708; RRID: IMSR_JAX:007914; RRID: SCR_003070NIH; RRID: AB_518614; RRID: AB_2298772; RRID: AB_10000240; RRID: AB_2079751; RRID: AB_2107133; RRID:SCR_002978

1. Introduction

The brain generates a robust and labile breathing pattern to maintain life and seamlessly integrates this rhythmic activity with daily activities, e.g., speech, exercise, and changes in physiological states, e.g., stress, fear. Moreover, this omnipresent rhythm could be utilized for modulating non-breathing related functions, such as cognition or emotion. Understanding how the brain controls breathing and coordinates it with other behaviors requires a high-resolution connectivity map of the participating neurons. The kernel for normal breathing rhythmogenesis, the preBötC, a small (<0.13mm^3 in rodents), bilateral cluster of ~3000 neurons in the ventrolateral medulla that generates rhythmic activity driving inspiratory breathing movements, is an opportune entry point.

Prior tracing studies broadly inform preBötC connectomics but lack subpopulation specificity, cf., (Tan, Pagliardini, Yang, Janczewski, & Feldman, 2010), as traditional tracers cannot separate projections of distinguishable cell types, e.g., excitatory vs. inhibitory, or

guarantee exclusive uptake by cell somas. We circumvented these limitations by exploiting transgenic mouse lines and virus-assisted mapping tools to examine projections of two genetically defined preBötC subpopulations: excitatory glutamatergic neurons expressing the peptide somatostatin (SST) that play an essential role in generating breathing pattern (Cui et al., 2016; Tan et al., 2008), and inhibitory neurons expressing the glycine transporter GlyT2, which modulate inspiratory pattern and generate apneas (Janczewski, Tashima, Hsu, Cui, & Feldman, 2013; Sherman, Worrell, Cui, & Feldman, 2015), although they are apparently not rhythmogenic (Cui et al., 2016; Sherman et al., 2015). Within rat brainstem, preBötC SST^+ neurons have extensive projections representing the structural core of the breathing CPG (Tan et al., 2010). Here, we delivered a Cre-dependent adeno-associated virus expressing EGFP (AAV-FLEX-EGFP) into the preBötC of SST-Cre mice and observed a similar projection pattern to breathing-related brainstem regions. In parallel, we identified projections of a subpopulation of inhibitory preBötC neurons in GlyT2-Cre mice. Given the different effects on breathing of manipulating the activity of preBötC excitatory and inhibitory neurons (Sherman et al., 2015; Tan et al., 2008), we hypothesized that these non-overlapping subpopulations of neurons would have distinct projection targets, though perhaps with some overlap. Strikingly, we found that both excitatory SST^+ and inhibitory glycinergic preBötC neurons send focal projections to all of the same brainstem nuclei. We examined overlapping projections in the pons and found that excitatory and inhibitory preBötC neurons can even innervate the same target neurons.

Although the primary role of the preBötC is widely accepted to be inspiratory rhythm generation driving inspiratory movements producing airflow ((Feldman, Del Negro, & Gray, 2013; Feldman & Kam, 2015), its rhythmic output may also serve other purposes, e.g., modulating emotion and higher-order behaviors such as arousal (Yackle et al., 2017) or even memory and fear (Zelano et al., 2016). While there are clear top-down influences on breathing, e.g., emotional (crying, laughing, etc.) (Guz, 1997) and volitional (speech, breath holding) breathing movements, there are reciprocal effects in humans, with breathing exercises during meditation, mindfulness, or yoga associated with improvements in cognitive processing, emotional state, and mood (Arch & Craske, 2006; Brown & Gerbarg, 2005; Jella & Shannahoff-Khalsa, 1993; Lockmann, Laplagne, Leao, & Tort, 2016; Zeidan, Johnson, Diamond, David, & Goolkasian, 2010; Zelano et al., 2016). Breathing rhythm is also a powerful force in shaping and coordinating other motor patterns, from fine orofacial movements, e.g., sniffing, whisking in rodents, and speech in humans, to large-scale movements such as running and swimming (Daley, Bramble, & Carrier, 2013; Kleinfeld, Deschenes, Wang, & Moore, 2014; Moore et al., 2013). Notably, such disparate functions as reaction times (Beh & Nix-James, 1974; Li, Park, & Borg, 2012) and pupillary diameter (Borgdorff, 1975; Ohtsuka, Asakura, Kawasaki, & Sawa, 1988) are modulated by the breathing cycle.

The relationship between breathing-related brainstem areas and suprapontine regions is not well understood, as previous circuit analyses of the breathing CPG have mostly been restricted to the brainstem and spinal cord. Direct suprapontine projection targets of the preBötC related to emotive and volitional control, especially limbic regions, have not been mapped comprehensively, particularly with respect to subpopulation-specific projections (Loewy, Wallach, & McKellar, 1981; Zagon, Totterdell, & Jones, 1994). We found that

preBötC neurons in mice projected to suprapontine regions not previously associated with breathing-modulated changes in blood gases and pH, including nuclei within the periaquaductal gray (PAG), thalamus, and hypothalamus. As with the brainstem projections, glutamatergic SST^+ and inhibitory $GlyT2^+$ preBötC neurons send parallel projections to the same suprapontine targets, suggesting that the preBötC is a source of direct inspiratory-modulated inputs that can affect emotional, cognitive, physiological, and behavioral functions.

2. Materials and Methods

Animals

Animal use was in accordance with the guidelines approved by the UCLA Institutional Animal Care and Use Committee. Mice were housed in a vivarium under a 12 hr light cycle with free access to food and water. All experiments were performed using adult male SST-Cre (IMSR Cat# JAX:013044, RRID: IMSR_JAX:013044), GlyT2-Cre, and GlyT2-EGFP mice (IMSR Cat# RBRC04708, RRID: IMSR_RBRC04708) (24–30 g) that were 10–24 weeks of age at the time of AAV injection. SST-Cre mice were crossed to Ai14 Cre-reporter mice (IMSR Cat# JAX:007914, RRID: IMSR_JAX:007914) to generate the SST reporter line used in retrograde tracing studies. Prior to surgery, mice were group housed in cages of up to 5 mice, and after surgery, mice were individually housed. GlyT2-Cre mice were kindly provided by H.U. Zeilhofer, University of Zurich, Switzerland, and all other mice were obtained from Jackson Labs (Bar Harbor, ME).

Surgical procedures

All experimental procedures were approved by the Chancellor's Animal Research Committee at the University of California, Los Angeles. For AAV iontophoresis injections, male mice (10–24 weeks old) were anesthetized with isoflurane and positioned in a stereotaxic apparatus (Kopf Instruments, Tujunga, CA). The skull was exposed with a midline scalp incision, and the stereotaxic frame was aligned at bregma using visual landmarks. A drill was placed over the skull at coordinates corresponding to the preBötC (anteroposterior, −6.78 mm; lateral, 1.25 mm) (Paxinos & Franklin, 2004), and a hole was drilled through the skull bone to expose the cerebellum. A micropipette (~20μm tip I.D.) loaded with virus (AAV-FLEX-EGFP; University of Pennsylvania Vector Core) was aligned at bregma (including in the z-axis), guided to the preBötC coordinates, and slowly lowered at 1 mm/min until it penetrated to a depth of −4.8 mm. A silver wire electrode was inserted into the micropipette, with the tip submerged in the viral solution, and was connected to a current source (Midgard Electronics, Watertown, MA). A current of 3μA (7 sec on, 7 sec off) was applied for 5 min, and the micropipette was left in place for 10 minutes to allow viral particles to diffuse and then withdrawn at 1 mm/min to minimize the backflow along the micropipette track. After surgery, mice were housed for 3 weeks to allow robust expression of EGFP.

For retrograde tracer experiments, Fluorogold™ (4% in saline) was injected into the amygdala (−1.20 mm anteroposterior, ±2.60 mm lateral, −4.25 mm ventral), cortex (0.90 mm anteroposterior, ±2.00 mm lateral and −2.80 mm ventral), LPO (0 mm anteroposterior,

±0.85 mm lateral, –4.75 mm ventral), thalamus (−1.95 mm anteroposterior, ±0.50 mm lateral, −2.85 mm ventral). SST and GlyT2-GFP reporter lines were injected to identify the molecular phenotype of retrogradely labeled preBötC neurons. Iontophoresis was performed as described above for AAV injection with an application of 3μA for 7 min. After surgery, mice were house for 6–8 days before their brains were processed for histology.

Histology

AAV-injected mice were processed for expression of EGFP as previously described (Sherman et al., 2015). Briefly, mice were deeply anesthetized with pentobarbital and perfused transcardially with saline followed by 4% paraformaldehyde in phosphate-buffered saline (PBS). Brains were removed, postfixed overnight at 4°C, and embedded in 3% Bactoagar. Free-floating coronal or sagittal sections (40 μm) were collected using a vibratome (Leica Biosystems, Buffalo Grove, IL) and stored at 4°C until further processing. Sections were incubated with primary antibodies in PBS containing 0.3% Triton X-100 (PBST) overnight at room temperature. After 3 washes, sections were incubated in species-appropriate secondary antibodies in PBST for 2h at room temperature. After 3 washes, sections were mounted onto gelatin-treated glass slides and coverslipped. Fluorescence was visualized with a confocal laser scanning microscope (LSM710; Carl Zeiss, Oberkochen, Germany). Images were acquired with Zen software (Carl Zeiss), exported as TIFF files, processed in Image J (NIH, Bethesda, MD; RRID: SCR_003070NIH), and prepared in Adobe Photoshop.

Antibody Characterization

We used the following primary antibodies: rabbit polyclonal anti-somatostatin-14 (T4103, 1:500; Peninsula Laboratories, San Carlos, CA), mouse monoclonal anti-NeuN (MAB377, 1:500; Millipore, Billerica, MA), chicken polyclonal anti-GFP (GFP-1020, 1:500; Aves Labs, Tigard, OR), goat polyclonal anti-choline acetyltransferase (AB144P, 1:500, Millipore), and sheep polyclonal anti-FoxP2 (AF5647, 1:16,000, R&D Systems, Minneapolis, MN). Secondary antibodies used were donkey anti-rabbit rhodamine Red-X, donkey anti-chicken DyLight488, donkey anti-mouse Cy5, and donkey anti-sheep rhodamine Red-X conjugated antibodies (1:250; Jackson ImmunoResearch, West Grove, PA).

Anti-somatostatin-14 antibody (Peninsula Laboratories, Cat# T-4103.0050, RRID: AB_518614) was raised in rabbit against the first 14 aa of the synthetic peptide SST. This antibody specifically recognizes SOM-14, SOM-28, SOM-25, and [Des-Ala^{1}]-SOM-14 in radioimmunoassay tests, and does not cross-react with other peptides such as substance P, amylin, glucagon, insulin, neuropeptide Y, and vasoactive intestinal peptide, or SST analogs according to the manufacturer. Preadsorption of the antibody with the SOM-14 peptide abolishes specific immunoreactivity in mouse brain sections (Scanlan, Dufourny, & Skinner, 2003).

The anti-NeuN antibody (Millipore, Cat# MAB377, RRID: AB_2298772) was raised in mice (clone A60) against the neuron-specific protein NeuN, which is expressed in most, but not all, neurons in the adult mouse brain, and not in glia (Mullen, Buck, & Smith, 1992).

The specificity of this antibody for neurons has been validated using immunohistochemistry and immunoblot analysis showing antibody binding to the nuclear fraction of brain tissue, but not other organs (Mullen et al., 1992).

Anti-GFP antibody (Aves Labs, Cat# GFP-1020, RRID: AB_10000240) was raised against recombinant EGFP in chickens, and the IgY fraction containing the antibody was affinity-purified from the yolks of immunized eggs. This anti-EGFP IgY specifically recognizes the viral-mediated EGFP-expressing neurons in adult rats (Tan et al., 2008; Tan et al., 2010). We did not observe immunolabeling in brain sections that were not infected by the virus expressing EGFP.

The anti-choline acetyltransferase (ChAT) antibody (Millipore, Cat# AB144P, RRID: AB_2079751) was raised in goat using the human placental enzyme as immunogen. Specificity of the antibody was verified by Western blotting in mouse brain lysate, where a single band corresponding to the 68–70 kDa ChAT protein was identified. In addition, immunolabeling in brain sections using this antibody was abolished after preincubation with rat recombinant choline acetyltransferase (Marquez-Ruiz, Morcuende, Navarro-Lopez Jde, & Escudero, 2007).

Sheep anti-FoxP2 antibody (R & D Systems, Cat# AF5647, RRID: AB_2107133) was raised against a recombinant peptide sequence from human FoxP2 (A640-E715) and affinity purified. Immunolabeling in the mouse brainstem using this primary antibody resulted in a pattern that is similar to *Foxp2* mRNA labeling as depicted in the Allen Brain Atlas (Allen Mouse Brain Atlas, RRID:SCR_002978; Geerling, Yokota, Rukhadze, Roe, & Chamberlin, 2017), and a Western blot from the manufacturer indicates that the antibody detects a single band at ~90 kDa corresponding to FoxP2 in human glioblastoma lysate.

Data analysis

For comparison of projection intensity between SST-Cre and GlyT2-Cre mice, EGFP-immunolabeled sections were imaged with a 20× objective. Images were converted to grayscale and pixel intensity was measured in the thalamus (NIH ImageJ) in 3 consecutive sections containing labeled projections. Noise was subtracted from the summed pixel values, providing an estimate of the projection intensity, and the fold difference between SST-Cre and GlyT2-Cre mice was calculated.

3. Results

Viral targeting of SST$^+$ and GlyT2$^+$ preBötC neurons

We identified projections of subpopulations of preBötC neurons to brainstem and suprapontine sites. The preBötC of SST-Cre and GlyT2-Cre mice were injected unilaterally with Cre-dependent AAV-FLEX-EGFP virus and given three weeks for EGFP to permeate throughout the somas and processes, particularly their axon terminal fields. Following histological processing (see METHODS), the preBötC was localized relative to clearly identifiable anatomical landmarks including facial and hypoglossal nuclei, and nucleus ambiguous, in conjunction with co-labeling for a molecular marker that labels subsets of preBötC neurons, i.e., SST (Fig 1; (Sherman et al., 2015)). EGFP-labeled cell bodies were

mostly restricted to the preBötC, with relatively few fluorescently-labeled neurons in surrounding regions, e.g., (Fig 1, bottom right). Experiments in which there was extensive EGFP expression along the micropipette track or in regions surrounding the preBötC were either excluded from analysis or used as controls to confirm that injections outside of the preBötC had a different projection profile compared to ones that encompassed the preBötC. Here we report the projections of preBötC neurons that were consistently observed across all experiments (n = 8 each SST-Cre and GlyT2-Cre) with clear, discrete projection fields.

Brainstem projections of preBötC neurons

SST^+ preBötC neurons projected to various well established components of the brainstem breathing CPG including the nucleus of the solitary tract (NTS), parahypoglossal region, i.e., the area surrounding the hypoglossal nucleus, rostral and caudal ventral respiratory group (rVRG; cVRG), Bötzinger Complex (BötC), RTN/pFRG, Kölliker-Fuse (KF), and parabrachial nuclei (Fig 2, top), as described previously in rats (Tan et al., 2010). These projections coursed dorsally to the parahypoglossal region and the NTS, laterally across the midline to the contralateral preBötC, with projections filling a spatial domain similar to that occupied by EGFP-labeled cell bodies on the injected side. Fluorescent processes radiated caudally to the rostral and caudal VRG, rostrally to the BötC, and dorsally to the region of the postulated post-inspiratory complex (PiCo; (Anderson et al., 2016)) both ipsi- and contralaterally. These neurons projected further rostrally to the: i) facial nucleus (VIIn); ii) lateral (parafacial lateral nucleus; pF_L) and ventral (parafacial ventral nucleus; pF_V) to VIIn (Huckstepp, Cardoza, Henderson, & Feldman, 2015) with processes that traversed through the intermediate reticular nucleus; iii) paratrigeminal region, but avoiding trigeminal nucleus motoneurons, and; iv) dorsolateral rostral pons, including KF and parabrachial nuclei.

Glycinergic preBötC neurons projected to the same regions as SST^+ neurons and the processes occupied the projection fields in a similar manner (Fig 2, bottom). The innervation of the $GlyT2^+$ neurons in GlyT2-Cre mice tended to be denser than that of SST^+ neurons in SST-Cre mice. This may be the consequence of more $GlyT2^+$ (~50% of inspiratory preBötC neurons) than SST^+ preBötC neurons (~10–20% of preBötC neurons) (Winter et al., 2009), consistent with our observation based on visual inspection that generally more preBötC neurons were transfected in GlyT2-Cre mice than in SST-Cre mice, despite the identical injection protocol.

While injections into the preBötC of both SST-Cre and GlyT2-Cre mice revealed strong projections to discrete nuclei, there were also markedly less dense and diffuse $EGFP^+$ processes that did not appear to target specific regions and are not described here. For example, we observed very sparse projections in the cerebellum and raphe nuclei, with a few projections in the locus coeruleus (cf., (Yackle et al., 2017) apparently straying from neighboring parabrachial nuclei.

Midbrain projections

SST^+ preBötC neurons projected robustly to the PAG and surrounding regions, as in rat (Tan et al., 2010), targeting the ventrolateral divisions in particular (Fig 3, top left). There were extensive projections to the inferior and superior colliculi (commissure, motor-related

region) and the midbrain reticular nucleus, within which were few diffuse projections in the ventral tegmental area (not shown). Interestingly, there were fibers clustered immediately dorsal to the substantia nigra pars compacta with a few extending into the nucleus.

As with the brainstem projections, glycinergic preBötC neurons also projected to similar regions as SST^+ preBötC neurons: the PAG (Fig 3, top right)., the inferior and superior colliculi, and midbrain reticular nucleus (not shown). Both SST^+ and $GlyT2^+$ processes had diffuse processes spanning much of the length of the midbrain, but for the most part appeared to be coursing through as fiber bundles.

Forebrain projections

As projections from transfected preBötC neurons traversed rostrally, $EGFP^+$ processes became sparser, with $EGFP^+$ arbors and puncta more readily observed. There were many thalamic nuclei that received projections from SST^+ preBötC neurons, including the subparafascicular nucleus, peripeduncular nucleus, and the ventral medial thalamic regions. The most distinct and specific projections were to the retroparafascicular nucleus, medial dorsal thalamic nucleus, and central medial thalamic nucleus (Fig 3, left). There were diffuse projections throughout large portions of the hypothalamus with concentrated projections in the posterior hypothalamus, the lateral hypothalamic area (LH), and the dorsal medial hypothalamus (DMH) (Fig 4, left). While sparse, there were also clear projections in the zona incerta, subthalamic nucleus, and substantia innominata (not shown). The most rostral projections were at the level of the preoptic hypothalamus, with few processes occasionally in and around the fornix. Few to no fibers were present in the suprachiasmatic nucleus, ventromedial hypothalamus, or arcuate nucleus. Well-defined projections were seen in the lateral preoptic area (LPO), with few sparse fibers in the medial preoptic nucleus, posterior bed nucleus of the stria terminals (Fig 4, left), and basal forebrain (not shown).

Within the forebrain as in the brainstem, $GlyT2^+$ preBötC neurons had a projection pattern similar to SST^+ preBötC neurons (Fig 4, right). For both SST^+ and $GlyT2^+$ preBötC neurons, projections were bilateral, with denser contralateral projections (Figs 3, 4). At level of the medial dorsal thalamus, contralateral projections were ~1.7 fold greater than ipsilateral projections (pixel intensity, n = 3). There were no substantial preBötC projections observed in the cortex, hippocampus, or olfactory bulb in either SST-Cre or GlyT2-Cre mice. In some mice (n=2/8 SST-Cre, 1/8 GlyT2), projections were present in the amygdala, but the fibers were sparse; since these projections were not reliably observed, we cannot conclude that the amygdala is a target of SST^+ or $GlyT2^+$ preBötC neurons.

All efferent target nuclei received overlapping projections from SST^+ and $GlyT2^+$ preBötC neurons. Both excitatory and inhibitory projections innervated regions bilaterally, but there were some regions that appeared to receive denser innervation on one side. Within the brainstem, ipsilateral projections from preBötC neurons were denser and more pronounced. For both SST^+ and $GlyT2^+$ neurons, projections to the midbrain were bilateral, but most suprapontine regions that received preBötC efferent projections were more strongly innervated contralateral to the injection site.

Retrograde tracing from suprapontine preBötC targets

To confirm the suprapontine efferent targets of preBötC neurons, we injected retrograde tracers into the observed (putative) projection sites to see if preBötC neurons were labeled. We made large injections of Fluorogold™ into two suprapontine projection targets of the preBötC: the LPO and central thalamus. For each region injected (either containing LPO or the central medial thalamus; n = 3 for each region) there was clear, consistent retrograde labeling of SST^+ and $GlyT2^+$ preBötC neurons (Fig 5), though at times sparse. Injections into the amygdala and piriform cortex, regions where we did not observe preBötC projections, did not retrogradely label preBötC neurons (n = 3 each, data not shown). These experiments confirmed that preBötC neurons indeed project directly to major suprapontine regions identified by viral tracing.

Excitatory and inhibitory preBötC neurons can innervate the same neuron

SST^+ and $GlyT2^+$ preBötC neurons project to the same target regions throughout the brain. Do their projections converge on individual neurons, or do they target distinct subpopulations? To explore this issue, we examined preBötC projections onto a subpopulation of dorsolateral parabrachial nucleus neurons that express the transcription factor FoxP2. In both SST-Cre and GlyT2-Cre mice injected with AAV-FLEX-EGFP, EGFP-labeled processes abutted the majority of these FoxP2 neurons (72 ± 20% SST-Cre mice; 63 ± 16% GlyT2-Cre mice, n = 3 each, Fig 6). Since more than 50% of these neurons were labeled in each case, at least some subset of the FoxP2 neurons within this region likely receive both excitatory and inhibitory input from the preBötC.

4. Discussion

The preBötC generates the rhythmic signals that underlie inspiratory breathing movement, as reflected in SST^+ and $GlyT2^+$ preBötC projections to the rostral and caudal VRG, which contain bulbospinal premotoneurons with mono- or oligosynaptic connections to motoneurons driving the phrenic, intercostal, and abdominal muscles (Alheid, Gray, Jiang, Feldman, & McCrimmon, 2002; Dobbins & Feldman, 1994; Hernandez, Lindsey, & Shannon, 1989), as well as to the parahypoglossal region, which contains premotoneurons projecting to vagal and hypoglossal motoneurons that control tongue and upper airway muscles (Chamberlin, Eikermann, Fassbender, White, & Malhotra, 2007; Dobbins & Feldman, 1995; Koizumi et al., 2008; Revill et al., 2015).

Reciprocal preBötC projections with brainstem breathing CPG allow feedback modulation

preBötC efferents target multiple brainstem breathing CPG nuclei that send reciprocal projections back to the preBötC, representing feedback loops capable of controlling and/or modulating breathing rhythm and pattern:

NTS—Part of a major sensory pathway, the NTS integrates and relays afferent signals from the vagal, facial, hypoglossal and glossopharyngeal nerves, and peripheral chemo-, baro- and stretch receptors (Zoccal, Furuya, Bassi, Colombari, & Colombari, 2014). The NTS conveys this information to the preBötC, among other brainstem regions, and suprapontine regions, projecting broadly to thalamus, hypothalamus, and limbic structures (Norgren, 1978).

BötC—Immediately rostral to the preBötC, the BötC is primarily composed of inhibitory glycinergic neurons (Ezure, Tanaka, & Kondo, 2003) and modulates inspiratory and expiratory timing (Jiang & Lipski, 1990). The BötC projects to the parabrachial nuclei, KF, NTS, VRG, and phrenic motoneurons (Ezure, Tanaka, & Saito, 2003; Fedorko & Merrill, 1984; Merrill & Fedorko, 1984; Tian, Peever, & Duffin, 1999).

pF—The pF_L is a presumptive essential partner of the preBötC, as it appears critical for generating expiratory motor activity driving expiratory airflow, i.e., active expiration (Huckstepp et al., 2015; Huckstepp, Henderson, Cardoza, & Feldman, 2016; Janczewski & Feldman, 2006; Pagliardini et al., 2011). The adjacent pF_V presumably acts as a CO_2/pH sensor, providing chemosensory drive to regulate breathing in response to metabolic demand. Projections dorsomedial to VIIn and BötC also labeled the region containing the recently identified PiCo, a region hypothesized to play a role in generating postinspiratory activity (Anderson et al., 2016).

Dorsolateral rostral pons—Different subtypes of neurons in the parabrachial nuclei and KF modulate inspiratory and expiratory duration, control the transition between inspiration to expiration, and may play a role in the generation of post-inspiratory activity (Dutschmann & Dick, 2012). The parabrachial nuclei and KF are reciprocally connected to many breathing CPG regions including VRG and NTS (Geerling et al., 2017; Yokota, Kaur, VanderHorst, Saper, & Chamberlin, 2015; Yokota, Oka, Tsumori, Nakamura, & Yasui, 2007). In addition to their reciprocal connectivity with the preBötC, these nuclei project rostrally to suprapontine regions including amygdala, cortex, bed nucleus of the stria terminalis, and hypothalamus (Krukoff, Harris, & Jhamandas, 1993), providing an ascending pathway for breathing-related signals to influence higher-order functions, including emotion and cognition.

Such extensive reciprocal interconnectivity with the rest of the breathing CPG enables the preBötC to generate a rhythm that can be highly regulated for physiological needs as well as affect non-breathing related functions and behaviors, e.g., metabolism, cognition, and emotion.

preBötC suprapontine projections transmit breathing-related signals that may modulate other behaviors or emotional state

PAG—The midbrain PAG is well-poised to integrate higher order sensory information with breathing during arousal, sleep, and emotional and defensive behaviors, e.g., fight or flight. The PAG receives descending information from limbic regions including cortex, central amygdala, thalamus, and hypothalamus (Beitz, 1982) and projects to various brainstem respiratory regions. PAG stimulation has diverse effects on breathing, e.g., slower and deeper breathing, and changes in respiratory timing, possibly through direct actions on the preBötC (Subramanian & Holstege, 2010, 2013)

Thalamus—preBötC projections to the thalamus represent a pathway for transmitting breathing information to the cortex. Breathing-modulated neurons are present in the thalamus (Chen, Eldridge, & Wagner, 1992). The parafascicular thalamic complex plays a

role in hypoxia-induced inhibition of breathing in the fetal brain (Koos et al., 2004; Koos, Rajaee, Ibe, Guerra, & Kruger, 2016). preBötC projections to the central medial thalamus, a region well connected to cortical, limbic, and sensorimotor structures including insular, anterior cingulate, somatosensory, and motor cortices, dorsal striatum, basolateral amygdala, nucleus accumbens, and basal ganglia (Vertes, Hoover, & Rodriguez, 2012), establishing a potential circuit to integrate breathing output with emotion and cognitive function. preBötC projections to the zona incerta, a nucleus implicated in coordinating corticothalamic and brainstem rhythms, motor function, and gating of pain, may serve a similar function.

Lateral and dorsomedial hypothalamus—These structures are implicated in feeding, reward, sleep/wakefulness, circadian rhythm, and stress (Saper, 2006; Stuber & Wise, 2016; Tyree & de Lecea, 2017). They contain orexin-producing neurons, some sensitive to CO_2 and pH (Williams, Jensen, Verkhratsky, Fugger, & Burdakov, 2007), that affect breathing across different states of arousal (Williams & Burdakov, 2008). Mice lacking orexin have a blunted ventilatory response to hypercapnia during wakefulness and increased apneas during sleep (Nakamura, Zhang, Yanagisawa, Fukuda, & Kuwaki, 2007), which may be mediated by interactions with the preBötC.

LPO—The LPO regulates arousal and motivated behaviors. LPO lesions increase wakefulness (Alam & Mallick, 1990), and local application of orexin- and melanin-concentrating hormone can affect sleep (Benedetto et al., 2013; Methippara, Alam, Szymusiak, & McGinty, 2000). LPO receives significant input from the nucleus accumbens and projects through the medial forebrain bundle to the pedunculopontine nucleus, the PAG and the superior colliculus, making the LPO part of the circuit by which limbic regions may modulate locomotor activity (Swanson, Mogenson, Gerfen, & Robinson, 1984). Thus, signals from the preBötC could modulate levels of arousal or activity.

Functional output of SST^+ and $GlyT2^+$ preBötC neurons

SST^+ preBötC neurons participate in generating the burst pattern that ultimately drives inspiratory motor output, and $GlyT2^+$ preBötC neurons modulate the respiratory pattern, but neither appear to be rhythmogenic (Cui et al., 2016; Sherman et al., 2015). SST^+ preBötC neurons are excitatory, unlike in other brain regions where SST is colocalized with GABA, i.e., non-preBötC SST^+ neurons are inhibitory, but the SST peptide, when released, is presumed to act as an inhibitory neuromodulator (Greene & Mason, 1996; Yamamoto, Runold, Prabhakar, Pantaleo, & Lagercrantz, 1988). Thus, the net effect of these preBötC neurons on their targets will be a function of the release patterns of glutamate and SST, which may be activity-dependent, as well as the receptor profile of the postsynaptic neurons. Given their phasic activity related to the breathing cycle, excitatory SST^+ and inhibitory $GlyT2^+$ preBötC neurons likely convey inspiratory-related signals to their targets. Even so, some projections may originate from non-inspiratory-modulated neurons in the preBötC or the bordering adjacent, i.e., rostral ventrolateral medulla, BötC, VRG, or reticular nucleus, and the functional output of such projections, if present, remains to be determined.

The convergence of SST^+ and $GlyT2^+$ projections onto the same brainstem and suprapontine regions, and in the dorsolateral parabrachial nucleus, even likely onto the same FoxP2

neurons, suggests that the magnitude and shape of breathing input to these regions is tightly controlled. For example, excitatory SST^+ neurons could signal cycle-by-cycle activity, while inhibitory glycinergic neurons could dampen (even eliminate) or sharpen this signal as needed; this balance of inhibition and excitation would enhance respiratory phase timing signals. Alternatively, excitatory and inhibitory projections could control different neuronal subpopulations working in parallel, opposition, or to perform distinct functions. For regions that are reciprocally connected with the preBötC, e.g., BötC, NTS, parabrachial nuclei, etc., this feedback could modulate preBötC intrinsic activity or output.

Input from the preBötC to brainstem and suprapontine regions may serve as a cycle-by-cycle efference copy of inspiratory activity to coordinate with or modulate other behaviors or physiological outputs. preBötC projections may provide continuous updates on breathing status for behaviors or physiological outputs that are critically timed to breathing cycle, e.g., cardiorespiratory coupling, speech/vocalizations, feeding, whisking, sniffing. Interestingly, we observed weak fibers broadly innervating the brainstem and midbrain, particularly regions that are responsible for sensorimotor integration, e.g., PAG. which could provide respiratory timing information wholesale or contribute to the synchronization of orofacial behaviors by the preBötC (Moore et al., 2013).

Other behaviors that may not require precise timing with the breathing cycle may instead be sensitive to acute changes in breathing pattern, as in exercise, response to stress, or significant homeostatic changes, e.g., body temperature. Breathing information from the preBötC could also be utilized across a longer timescale to affect sleep (Mortola, 2004). preBötC projections to rostral suprapontine regions could function to match propriosensory feedback with motor information about breathing status to affect the volitional or emotional modulation of breathing. In humans, the ability to monitor ventilatory status and generate (or mask) the sensory percept of breathing is thought to arise through the gating of sensorimotor and proprioceptive feedback from breathing pathways, possibly through thalamus or hippocampus, to the cortex (Davenport & Vovk, 2009). Under eupneic conditions, the cortex may not register breathing rhythm on a cycle-by-cycle basis. However, given a strong stimulus, i.e., dyspnea or breathing distress, the resulting breathing-related sensory signals could break through to higher cortical and limbic areas as a breathing sensation with an emotional valence, e.g., anxiety, panic. Moreover, direct signals from breathing CPG efferents to suprapontine regions could contribute to dysfunctions in the perception of breathing, e.g., breathlessness (Banzett et al., 2000; Davenport & Vovk, 2009; Kinkead, Tenorio, Drolet, Bretzner, & Gargaglioni, 2014)

Is breathing connected to emotions and cognition?

Though breathing is intimately linked to emotions and cognition, how signals related to breathing are registered in higher brain centers that process emotions or cognitive functions is unknown. Although we identified direct projections from SST^+ or $GlyT2^+$ preBötC neurons to the thalamus and hypothalamus, we did not find robust projections to regions associated with emotions and cognition, e.g., amygdala, hippocampus, or cortex. Thus, perhaps only a few preBötC neurons project to these regions, projections may be difficult to detect due to insufficient labeling, i.e., false negatives, or the neurons projecting to these

regions are not proper preBötC neurons, but lie in the preBötC surround. Furthermore, in such instances where projections to specific regions were labeled in only a few cases and not further examined, there may be projections originating from undefined subsets of SST^+ or $GlyT2^+$ preBötC neurons with potential subtle differences in projection profiles between the two populations. Alternatively, direct projections to limbic areas may originate from a non-SST, non-GlyT2 preBötC neuronal subtype. SST^+ neurons comprise ~17% of preBötC excitatory neurons (Gray et al., 2010), and $GlyT2^+$ neurons nearly half of the inspiratory-related preBötC inhibitory neurons, leaving a substantial fraction of preBötC neurons unmapped. Populations of interest include neurons derived from the precursors expressing Dbx1, of which SST^+ neurons are only a subset. This is likely of significance, as our recent work suggests that $Dbx1^+SST^-$ neurons are candidates for the rhythmogenic subset of excitatory neurons (Cui et al., 2016). While these neurons likely project locally within the preBötC microcircuit, they may project to other regions, perhaps distinct from SST^+ neurons. A smaller subset of preBötC neurons that express the molecular marker Cdh9, which do not overlap with SST^+ neurons, project to locus coeruleus (a projection we did not observe), a major center relaying information rostrally that appears to modulate calm and arousal (Yackle et al., 2017). GABAergic neurons, while overlapping with glycinergic neurons, may also provide a separate projection pattern.

Breathing information from the preBötC need not be monosynaptic to suprapontine targets, e.g., amygdala, hippocampus, or cortex; indeed, it can readily be relayed via ascending projections through intermediate nuclei that in turn project directly to these targets. Potential intermediaries include parabrachial nuclei and NTS (Benarroch, 2016), which receive dense projections from the preBötC and project broadly to the thalamus, hypothalamus, and amygdala (Saper & Loewy, 1980), as well as locus coeruleus (Yackle et al., 2017). Breathing-related signals may also be indirectly transmitted to higher-order brain regions via sensory afferent feedback, e.g., breathing-related pulmonary vagal afferents or through breathing-modulated olfactory bulb activity, effectively bypassing the preBötC. Both the hippocampus and limbic regions, including cortex and amygdala, exhibit distinct breathing-related oscillations: in rats, such synchrony is hypothesized to link olfaction with memory and learning (Lockmann et al., 2016); in humans, breathing rhythm entrains oscillatory activity in the piriform cortex, amygdala, and hippocampus and may improve cognitive and emotional processing in a respiratory phase-dependent manner (Zelano et al., 2016). Thus, the preBötC generates rhythmic activity that entrains other behaviors, e.g., sniffing and whisking, and can phase lock with or underlie oscillations in the higher-order brain regions important for cognition and emotion.

We established extensive preBötC connectivity throughout the brain, with excitatory and inhibitory neurons projecting to other central components of the brainstem breathing CPG and suprapontine regions through direct or second-order pathways, which we hypothesize modulate emotional and cognitive processes or coordinate behaviors (Fig 7). This highlights the importance of the preBötC not only as the kernel of the breathing CPG, but also as a central source of breathing output that is distributed widely across the brain with likely far reaching effects.

Acknowledgments

The authors would like to thank Lauren Henderson, Sarah Heath, and Grace Li for excellent technical assistance. This work was supported by the A.P. Giannini Foundation (CFY) and the National Institutes of Health (NIH F32 HL126522 (CFY), RO1 NS72211, and R35 HL135779 (JLF)).

References

Alam MN, Mallick BN. Differential acute influence of medial and lateral preoptic areas on sleep-wakefulness in freely moving rats. Brain Res. 1990; 525(2):242–248. [PubMed: 2253029]

Alheid GF, Gray PA, Jiang MC, Feldman JL, McCrimmon DR. Parvalbumin in respiratory neurons of the ventrolateral medulla of the adult rat. J Neurocytol. 2002; 31(8–9):693–717. [PubMed: 14501208]

Anderson TM, Garcia AJ 3rd, Baertsch NA, Pollak J, Bloom JC, Wei AD, Rai KG, Ramirez JM. A novel excitatory network for the control of breathing. Nature. 2016; 536(7614):76–80. DOI: 10.1038/nature18944 [PubMed: 27462817]

Arch JJ, Craske MG. Mechanisms of mindfulness: emotion regulation following a focused breathing induction. Behav Res Ther. 2006; 44(12):1849–1858. DOI: 10.1016/j.brat.2005.12.007 [PubMed: 16460668]

Banzett RB, Mulnier HE, Murphy K, Rosen SD, Wise RJ, Adams L. Breathlessness in humans activates insular cortex. Neuroreport. 2000; 11(10):2117–2120. [PubMed: 10923655]

Beh HC, Nix-James DR. The relationship between respiration phase and reaction time. Psychophysiology. 1974; 11(3):400–401. [PubMed: 4423726]

Beitz AJ. The organization of afferent projections to the midbrain periaqueductal gray of the rat. Neuroscience. 1982; 7(1):133–159. [PubMed: 7078723]

Benarroch EE. Parabrachial nuclear complex: Multiple functions and potential clinical implications. Neurology. 2016; 86(7):676–683. DOI: 10.1212/WNL.0000000000002393 [PubMed: 26791152]

Benedetto L, Rodriguez-Servetti Z, Lagos P, D'Almeida V, Monti JM, Torterolo P. Microinjection of melanin concentrating hormone into the lateral preoptic area promotes non-REM sleep in the rat. Peptides. 2013; 39:11–15. DOI: 10.1016/j.peptides.2012.10.005 [PubMed: 23123302]

Borgdorff P. Respiratory fluctuations in pupil size. Am J Physiol. 1975; 228(4):1094–1102. [PubMed: 1130509]

Brown RP, Gerbarg PL. Sudarshan Kriya Yogic breathing in the treatment of stress, anxiety, and depression. Part II--clinical applications and guidelines. J Altern Complement Med. 2005; 11(4): 711–717. DOI: 10.1089/acm.2005.11.711 [PubMed: 16131297]

Chamberlin NL, Eikermann M, Fassbender P, White DP, Malhotra A. Genioglossus premotoneurons and the negative pressure reflex in rats. J Physiol. 2007; 579(Pt 2):515–526. DOI: 10.1113/jphysiol.2006.121889 [PubMed: 17185342]

Chen Z, Eldridge FL, Wagner PG. Respiratory-associated thalamic activity is related to level of respiratory drive. Respir Physiol. 1992; 90(1):99–113. [PubMed: 1455102]

Cui Y, Kam K, Sherman D, Janczewski WA, Zheng Y, Feldman JL. Defining preBotzinger Complex Rhythm- and Pattern-Generating Neural Microcircuits In Vivo. Neuron. 2016; 91(3):602–614. DOI: 10.1016/j.neuron.2016.07.003 [PubMed: 27497222]

Daley MA, Bramble DM, Carrier DR. Impact loading and locomotor-respiratory coordination significantly influence breathing dynamics in running humans. PLoS One. 2013; 8(8):e70752.doi: 10.1371/journal.pone.0070752 [PubMed: 23950997]

Davenport PW, Vovk A. Cortical and subcortical central neural pathways in respiratory sensations. Respir Physiol Neurobiol. 2009; 167(1):72–86. DOI: 10.1016/j.resp.2008.10.001 [PubMed: 18977463]

Dobbins EG, Feldman JL. Brainstem network controlling descending drive to phrenic motoneurons in rat. J Comp Neurol. 1994; 347(1):64–86. [PubMed: 7798382]

Dobbins EG, Feldman JL. Differential innervation of protruder and retractor muscles of the tongue in rat. J Comp Neurol. 1995; 357(3):376–394. [PubMed: 7673474]

Dutschmann M, Dick TE. Pontine mechanisms of respiratory control. Compr Physiol. 2012; 2(4): 2443–2469. DOI: 10.1002/cphy.c100015 [PubMed: 23720253]

Ezure K, Tanaka I, Kondo M. Glycine is used as a transmitter by decrementing expiratory neurons of the ventrolateral medulla in the rat. J Neurosci. 2003; 23(26):8941–8948. [PubMed: 14523096]

Ezure K, Tanaka I, Saito Y. Brainstem and spinal projections of augmenting expiratory neurons in the rat. Neurosci Res. 2003; 45(1):41–51. [PubMed: 12507723]

Fedorko L, Merrill EG. Axonal projections from the rostral expiratory neurones of the Botzinger complex to medulla and spinal cord in the cat. J Physiol. 1984; 350:487–496. [PubMed: 6747857]

Feldman JL, Del Negro CA, Gray PA. Understanding the rhythm of breathing: so near, yet so far. Annu Rev Physiol. 2013; 75:423–452. DOI: 10.1146/annurev-physiol-040510-130049 [PubMed: 23121137]

Feldman JL, Kam K. Facing the challenge of mammalian neural microcircuits: taking a few breaths may help. J Physiol. 2015; 593(1):3–23. DOI: 10.1113/jphysiol.2014.277632 [PubMed: 25556783]

Geerling JC, Yokota S, Rukhadze I, Roe D, Chamberlin NL. Kolliker-Fuse GABAergic and glutamatergic neurons project to distinct targets. J Comp Neurol. 2017; 525(8):1844–1860. DOI: 10.1002/cne.24164 [PubMed: 28032634]

Gray PA, Hayes JA, Ling GY, Llona I, Tupal S, Picardo MC, Ross SE, Hirata T, Corbin JG, Eugenín J, Del Negro CA. Developmental origin of preBotzinger complex respiratory neurons. J Neurosci. 2010; 30(44):14883–14895. DOI: 10.1523/JNEUROSCI.4031-10.2010 [PubMed: 21048147]

Greene JR, Mason A. Effects of somatostatin and related peptides on the membrane potential and input resistance of rat ventral subicular neurons, in vitro. J Pharmacol Exp Ther. 1996; 276(2):426–432. [PubMed: 8632306]

Guz A. Brain, breathing and breathlessness. Respir Physiol. 1997; 109(3):197–204. [PubMed: 9342797]

Hernandez YM, Lindsey BG, Shannon R. Intercostal and abdominal muscle afferent influence on caudal medullary expiratory neurons that drive abdominal muscles. Exp Brain Res. 1989; 78(1): 219–222. [PubMed: 2531680]

Huckstepp RT, Cardoza KP, Henderson LE, Feldman JL. Role of parafacial nuclei in control of breathing in adult rats. J Neurosci. 2015; 35(3):1052–1067. DOI: 10.1523/JNEUROSCI. 2953-14.2015 [PubMed: 25609622]

Huckstepp RT, Henderson LE, Cardoza KP, Feldman JL. Interactions between respiratory oscillators in adult rats. Elife. 2016; 5doi: 10.7554/eLife.14203

Janczewski WA, Feldman JL. Distinct rhythm generators for inspiration and expiration in the juvenile rat. J. Physiol. 2006; 570(Pt 2):407–420. DOI: 10.1113/jphysiol.2005.098848 [PubMed: 16293645]

Janczewski WA, Tashima A, Hsu P, Cui Y, Feldman JL. Role of inhibition in respiratory pattern generation. J Neurosci. 2013; 33(13):5454–5465. DOI: 10.1523/JNEUROSCI.1595-12.2013 [PubMed: 23536061]

Jella SA, Shannahoff-Khalsa DS. The effects of unilateral forced nostril breathing on cognitive performance. Int J Neurosci. 1993; 73(1–2):61–68. [PubMed: 8132419]

Jiang C, Lipski J. Extensive monosynaptic inhibition of ventral respiratory group neurons by augmenting neurons in the Botzinger complex in the cat. Exp Brain Res. 1990; 81(3):639–648. [PubMed: 2226695]

Kinkead R, Tenorio L, Drolet G, Bretzner F, Gargaglioni L. Respiratory manifestations of panic disorder in animals and humans: a unique opportunity to understand how supramedullary structures regulate breathing. Respir Physiol Neurobiol. 2014; 204:3–13. DOI: 10.1016/j.resp. 2014.06.013 [PubMed: 25038523]

Kleinfeld D, Deschenes M, Wang F, Moore JD. More than a rhythm of life: breathing as a binder of orofacial sensation. Nat Neurosci. 2014; 17(5):647–651. DOI: 10.1038/nn.3693 [PubMed: 24762718]

Koizumi H, Wilson CG, Wong S, Yamanishi T, Koshiya N, Smith JC. Functional imaging, spatial reconstruction, and biophysical analysis of a respiratory motor circuit isolated in vitro. J Neurosci. 2008; 28(10):2353–2365. DOI: 10.1523/JNEUROSCI.3553-07.2008 [PubMed: 18322082]

Koos BJ, Kawasaki Y, Hari A, Bohorquez F, Jan C, Roostaeian J, Wilson CL, Kruger L. Electrical stimulation of the posteromedial thalamus modulates breathing in unanesthetized fetal sheep. J Appl Physiol (1985). 2004; 96(1):115–123. DOI: 10.1152/japplphysiol.00517.2003 [PubMed: 14660492]

Koos BJ, Rajaee A, Ibe B, Guerra C, Kruger L. Thalamic mediation of hypoxic respiratory depression in lambs. Am J Physiol Regul Integr Comp Physiol. 2016; 310(7):R586–595. DOI: 10.1152/ajpregu.00412.2015 [PubMed: 26818057]

Krukoff TL, Harris KH, Jhamandas JH. Efferent projections from the parabrachial nucleus demonstrated with the anterograde tracer Phaseolus vulgaris leucoagglutinin. Brain Res Bull. 1993; 30(1–2):163–172. [PubMed: 7678381]

Li S, Park WH, Borg A. Phase-dependent respiratory-motor interactions in reaction time tasks during rhythmic voluntary breathing. Motor Control. 2012; 16(4):493–505. [PubMed: 22643317]

Lockmann AL, Laplagne DA, Leao RN, Tort AB. A Respiration-Coupled Rhythm in the Rat Hippocampus Independent of Theta and Slow Oscillations. J Neurosci. 2016; 36(19):5338–5352. DOI: 10.1523/JNEUROSCI.3452-15.2016 [PubMed: 27170130]

Loewy AD, Wallach JH, McKellar S. Efferent connections of the ventral medulla oblongata in the rat. Brain Res. 1981; 228(1):63–80. [PubMed: 7023615]

Marquez-Ruiz J, Morcuende S, Navarro-Lopez Jde D, Escudero M. Anatomical and pharmacological relationship between acetylcholine and nitric oxide in the prepositus hypoglossi nucleus of the cat: functional implications for eye-movement control. J Comp Neurol. 2007; 503(3):407–420. DOI: 10.1002/cne.21397 [PubMed: 17503470]

Merrill EG, Fedorko L. Monosynaptic inhibition of phrenic motoneurons: a long descending projection from Botzinger neurons. J Neurosci. 1984; 4(9):2350–2353. [PubMed: 6090616]

Methippara MM, Alam MN, Szymusiak R, McGinty D. Effects of lateral preoptic area application of orexin-A on sleep-wakefulness. Neuroreport. 2000; 11(16):3423–3426. [PubMed: 11095491]

Moore JD, Deschenes M, Furuta T, Huber D, Smear MC, Demers M, Kleinfeld D. Hierarchy of orofacial rhythms revealed through whisking and breathing. Nature. 2013; 497(7448):205–210. DOI: 10.1038/nature12076 [PubMed: 23624373]

Mortola JP. Breathing around the clock: an overview of the circadian pattern of respiration. Eur J Appl Physiol. 2004; 91(2–3):119–129. DOI: 10.1007/s00421-003-0978-0 [PubMed: 14569400]

Mullen RJ, Buck CR, Smith AM. NeuN, a neuronal specific nuclear protein in vertebrates. Development. 1992; 116(1):201–211. [PubMed: 1483388]

Nakamura A, Zhang W, Yanagisawa M, Fukuda Y, Kuwaki T. Vigilance state-dependent attenuation of hypercapnic chemoreflex and exaggerated sleep apnea in orexin knockout mice. J Appl Physiol (1985). 2007; 102(1):241–248. DOI: 10.1152/japplphysiol.00679.2006 [PubMed: 16959906]

Norgren R. Projections from the nucleus of the solitary tract in the rat. Neuroscience. 1978; 3(2):207–218. [PubMed: 733004]

Ohtsuka K, Asakura K, Kawasaki H, Sawa M. Respiratory fluctuations of the human pupil. Exp Brain Res. 1988; 71(1):215–217. [PubMed: 3416953]

Pagliardini S, Janczewski WA, Tan W, Dickson CT, Deisseroth K, Feldman JL. Active expiration induced by excitation of ventral medulla in adult anesthetized rats. J. Neurosci. 2011; 31(8):2895–2905. DOI: 10.1523/JNEUROSCI.5338-10.2011 [PubMed: 21414911]

Paxinos, G., Franklin, KBJ. The mouse brain in stereotaxic coordinates. 2. Amsterdam ; Boston: Elsevier Academic Press; 2004. Compact

Revill AL, Vann NC, Akins VT, Kottick A, Gray PA, Del Negro CA, Funk GD. Dbx1 precursor cells are a source of inspiratory XII premotoneurons. Elife. 2015; 4doi: 10.7554/eLife.12301

Saper CB. Staying awake for dinner: hypothalamic integration of sleep, feeding, and circadian rhythms. Progress in Brain Research. 2006; 153:243–252. DOI: 10.1016/S0079-6123(06)53014-6 [PubMed: 16876579]

Saper CB, Loewy AD. Efferent connections of the parabrachial nucleus in the rat. Brain Res. 1980; 197(2):291–317. [PubMed: 7407557]

Scanlan N, Dufourny L, Skinner DC. Somatostatin-14 neurons in the ovine hypothalamus: colocalization with estrogen receptor alpha and somatostatin-28(1–12) immunoreactivity, and

activation in response to estradiol. Biol Reprod. 2003; 69(4):1318–1324. DOI: 10.1095/biolreprod.103.017848 [PubMed: 12773414]

Sherman D, Worrell JW, Cui Y, Feldman JL. Optogenetic perturbation of preBotzinger complex inhibitory neurons modulates respiratory pattern. Nat Neurosci. 2015; doi: 10.1038/nn.3938

Stuber GD, Wise RA. Lateral hypothalamic circuits for feeding and reward. Nat Neurosci. 2016; 19(2): 198–205. DOI: 10.1038/nn.4220 [PubMed: 26814589]

Subramanian HH, Holstege G. Periaqueductal gray control of breathing. Adv Exp Med Biol. 2010; 669:353–358. DOI: 10.1007/978-1-4419-5692-7_72 [PubMed: 20217381]

Subramanian HH, Holstege G. Stimulation of the midbrain periaqueductal gray modulates preinspiratory neurons in the ventrolateral medulla in the rat in vivo. J Comp Neurol. 2013; 521(13):3083–3098. DOI: 10.1002/cne.23334 [PubMed: 23630049]

Swanson LW, Mogenson GJ, Gerfen CR, Robinson P. Evidence for a projection from the lateral preoptic area and substantia innominata to the 'mesencephalic locomotor region' in the rat. Brain Res. 1984; 295(1):161–178. [PubMed: 6201228]

Tan W, Janczewski WA, Yang P, Shao XM, Callaway EM, Feldman JL. Silencing preBötzinger complex somatostatin-expressing neurons induces persistent apnea in awake rat. Nat. Neurosci. 2008; 11(5):538–540. DOI: 10.1038/nn.2104 [PubMed: 18391943]

Tan W, Pagliardini S, Yang P, Janczewski WA, Feldman JL. Projections of preBötzinger complex neurons in adult rats. J. Comp. Neurol. 2010; 518(10):1862–1878. DOI: 10.1002/cne.22308 [PubMed: 20235095]

Tian GF, Peever JH, Duffin J. Botzinger-complex, bulbospinal expiratory neurones monosynaptically inhibit ventral-group respiratory neurones in the decerebrate rat. Exp Brain Res. 1999; 124(2): 173–180. [PubMed: 9928840]

Tyree SM, de Lecea L. Lateral Hypothalamic Control of the Ventral Tegmental Area: Reward Evaluation and the Driving of Motivated Behavior. Front Syst Neurosci. 2017; 11:50.doi: 10.3389/fnsys.2017.00050 [PubMed: 28729827]

Vertes RP, Hoover WB, Rodriguez JJ. Projections of the central medial nucleus of the thalamus in the rat: node in cortical, striatal and limbic forebrain circuitry. Neuroscience. 2012; 219:120–136. DOI: 10.1016/j.neuroscience.2012.04.067 [PubMed: 22575585]

Williams RH, Burdakov D. Hypothalamic orexins/hypocretins as regulators of breathing. Expert Rev Mol Med. 2008; 10:e28.doi: 10.1017/S1462399408000823 [PubMed: 18828950]

Williams RH, Jensen LT, Verkhratsky A, Fugger L, Burdakov D. Control of hypothalamic orexin neurons by acid and CO2. Proc Natl Acad Sci U S A. 2007; 104(25):10685–10690. DOI: 10.1073/pnas.0702676104 [PubMed: 17563364]

Winter SM, Fresemann J, Schnell C, Oku Y, Hirrlinger J, Hulsmann S. Glycinergic interneurons are functionally integrated into the inspiratory network of mouse medullary slices. Pflugers Arch. 2009; 458(3):459–469. DOI: 10.1007/s00424-009-0647-1 [PubMed: 19238427]

Yackle K, Schwarz LA, Kam K, Sorokin JM, Huguenard JR, Feldman JL, Luo L, Krasnow MA. Breathing control center neurons that promote arousal in mice. Science. 2017; 355(6332):1411–1415. DOI: 10.1126/science.aai7984 [PubMed: 28360327]

Yamamoto Y, Runold M, Prabhakar N, Pantaleo T, Lagercrantz H. Somatostatin in the control of respiration. Acta Physiol Scand. 1988; 134(4):529–533. DOI: 10.1111/j.1748-1716.1998.tb08527.x [PubMed: 2907961]

Yokota S, Kaur S, VanderHorst VG, Saper CB, Chamberlin NL. Respiratory-related outputs of glutamatergic, hypercapnia-responsive parabrachial neurons in mice. J Comp Neurol. 2015; 523(6):907–920. DOI: 10.1002/cne.23720 [PubMed: 25424719]

Yokota S, Oka T, Tsumori T, Nakamura S, Yasui Y. Glutamatergic neurons in the Kolliker-Fuse nucleus project to the rostral ventral respiratory group and phrenic nucleus: a combined retrograde tracing and in situ hybridization study in the rat. Neurosci Res. 2007; 59(3):341–346. DOI: 10.1016/j.neures.2007.08.004 [PubMed: 17888537]

Zagon A, Totterdell S, Jones RS. Direct projections from the ventrolateral medulla oblongata to the limbic forebrain: anterograde and retrograde tract-tracing studies in the rat. J Comp Neurol. 1994; 340(4):445–468. DOI: 10.1002/cne.903400402 [PubMed: 7516349]

Zeidan F, Johnson SK, Diamond BJ, David Z, Goolkasian P. Mindfulness meditation improves cognition: evidence of brief mental training. Conscious Cogn. 2010; 19(2):597–605. DOI: 10.1016/j.concog.2010.03.014 [PubMed: 20363650]

Zelano C, Jiang H, Zhou G, Arora N, Schuele S, Rosenow J, Gottfried JA. Nasal Respiration Entrains Human Limbic Oscillations and Modulates Cognitive Function. J Neurosci. 2016; 36(49):12448–12467. DOI: 10.1523/JNEUROSCI.2586-16.2016 [PubMed: 27927961]

Zoccal DB, Furuya WI, Bassi M, Colombari DS, Colombari E. The nucleus of the solitary tract and the coordination of respiratory and sympathetic activities. Front Physiol. 2014; 5:238.doi: 10.3389/fphys.2014.00238 [PubMed: 25009507]

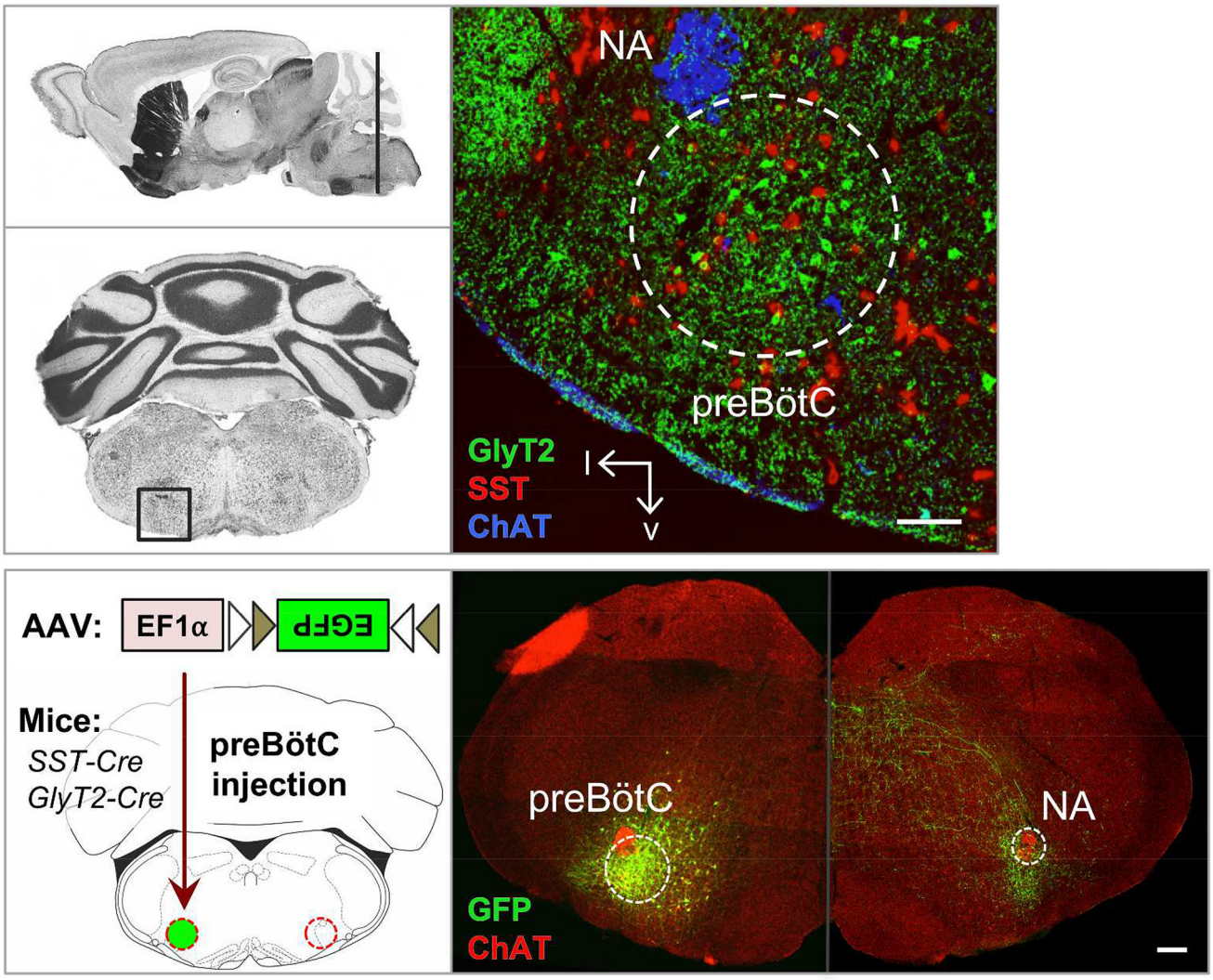

Figure 1.

AAV targeting of the preBötC. Top: Nissl stained sagittal and coronal sections (Paxinos & Franklin, 2004) at the level of the preBötC (dark line and boxed, left) and localization of preBötC via anatomical landmarks and markers for GlyT2 (green), SST (red), and ChAT (blue). NA, nucleus ambiguous. Scale bar = 100 μm. Bottom: Schematic of AAV strategy. Injection of Cre-dependent AAV-FLEX-EGFP into the preBötC of SST- or GlyT2-Cre lines leads to localized expression of EGFP. AAV injection into GlyT2-Cre mouse leads to robust expression in the cell bodies (left half) as well as processes, allowing identification of efferent projections (right half, brightness enhanced). Scale bar = 200μm

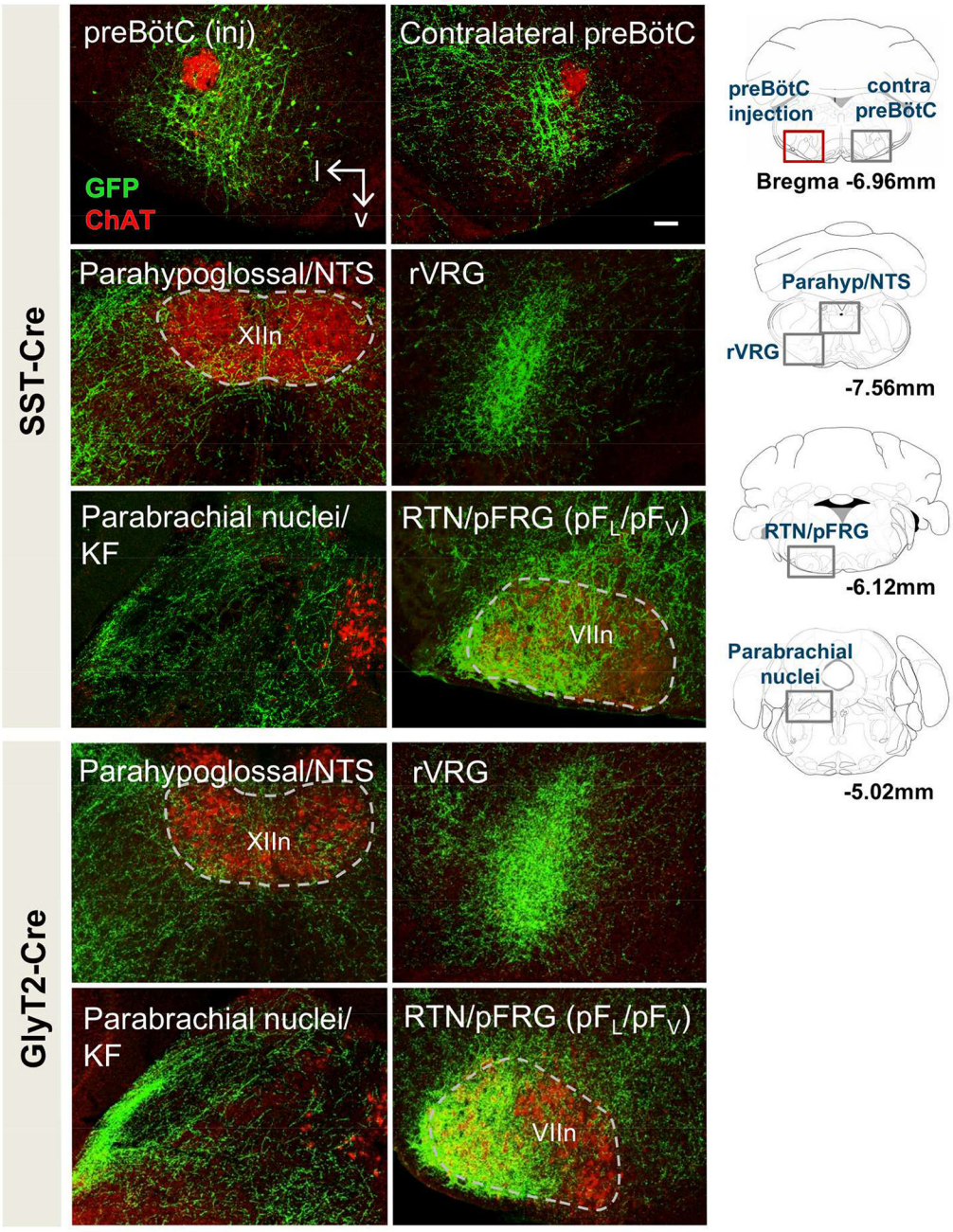

Figure 2.

Brainstem projections of SST$^+$ (top) and GlyT2$^+$ (bottom) preBötC neurons. Top: Projections of SST$^+$ neurons extend to the contralateral preBötC, the ventral respiratory group (VRG) parahypoglossal/NTS, parabrachial nuclei/KF as well as the RTN/pFRG (pF$_L$/pF$_V$). Bottom: GlyT2$^+$ preBötC projections extend to the same regions. Location of each image indicated as gray boxes in the schematics to the right; preBötC injection site in red. Scale bar = 100μm.

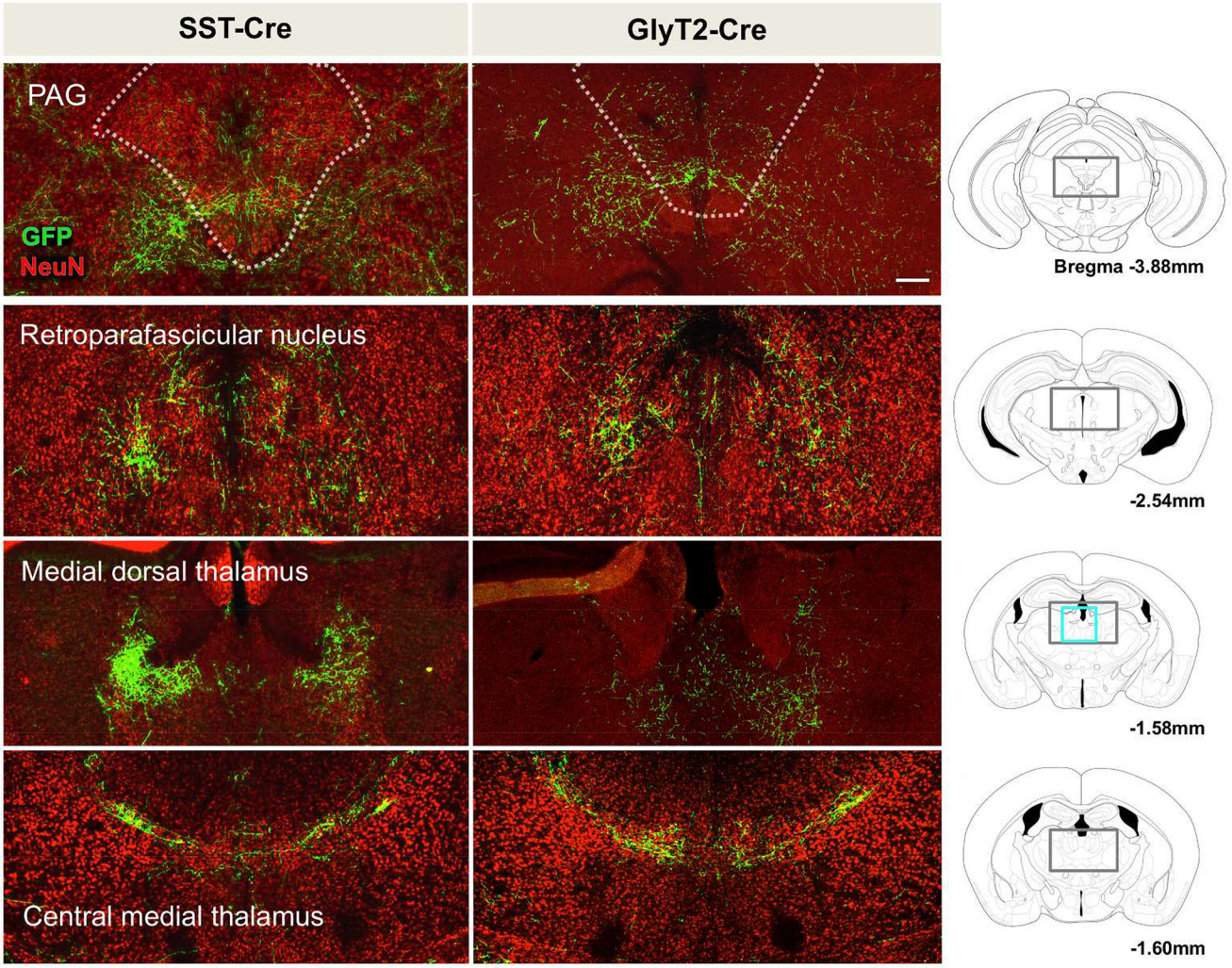

Figure 3.

Projections of SST$^+$ (left) and GlyT2$^+$ (right) preBötC neurons extend to the midbrain PAG and various thalamic nuclei, including the retroparafascicular, medial dorsal, and central medial thalamic nuclei (EGFP$^+$ processes in green, neuronal marker NeuN in red). Gray boxes in schematic represent location of images shown. Scale bar = 200μm.

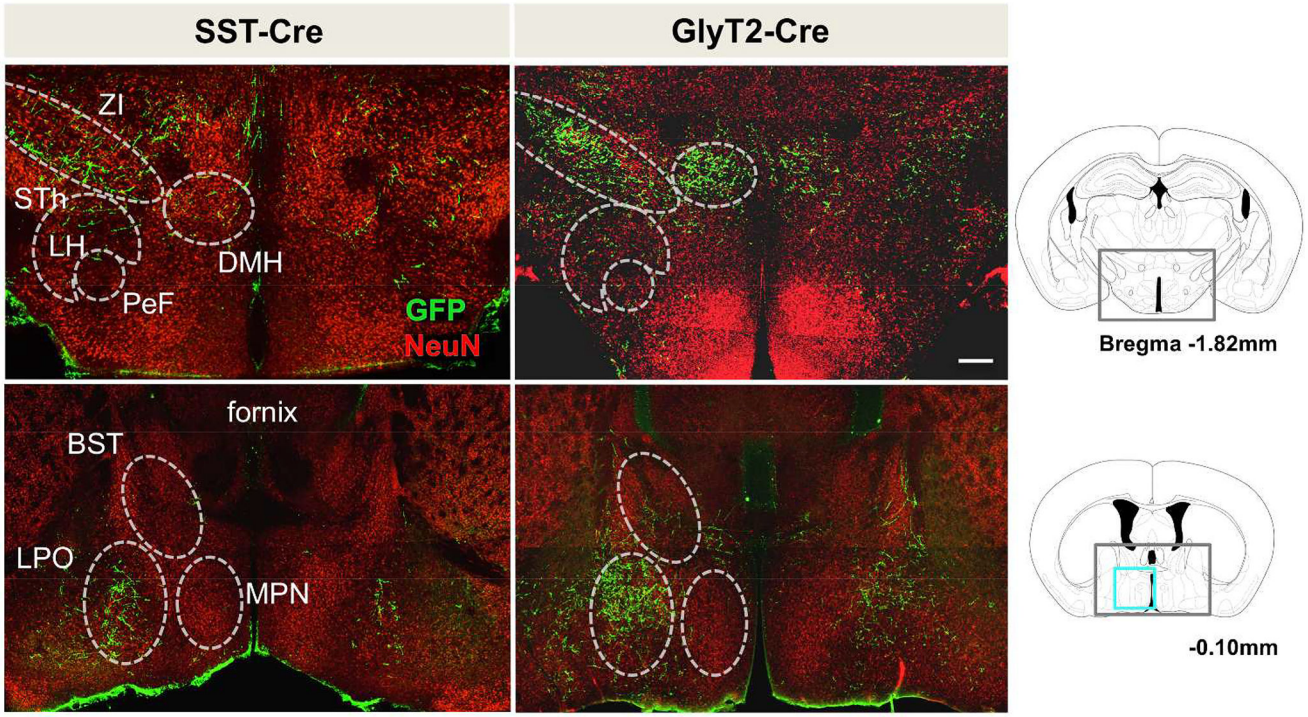

Figure 4.

Suprapontine projections of SST^{+} (left) and $GlyT2^{+}$ (right) preBötC neurons extend to the zona incerta (ZI), lateral (LH) and dorsomedial hypothalamus (DMH) as well as the lateral preoptic area (LPO). Gray boxes in schematic represent location of images shown. (STh, subthalamic nucleus; BST, bed nucleus of the stria terminalis; MPN, medial preoptic nucleus) Scale bar = 200μm.

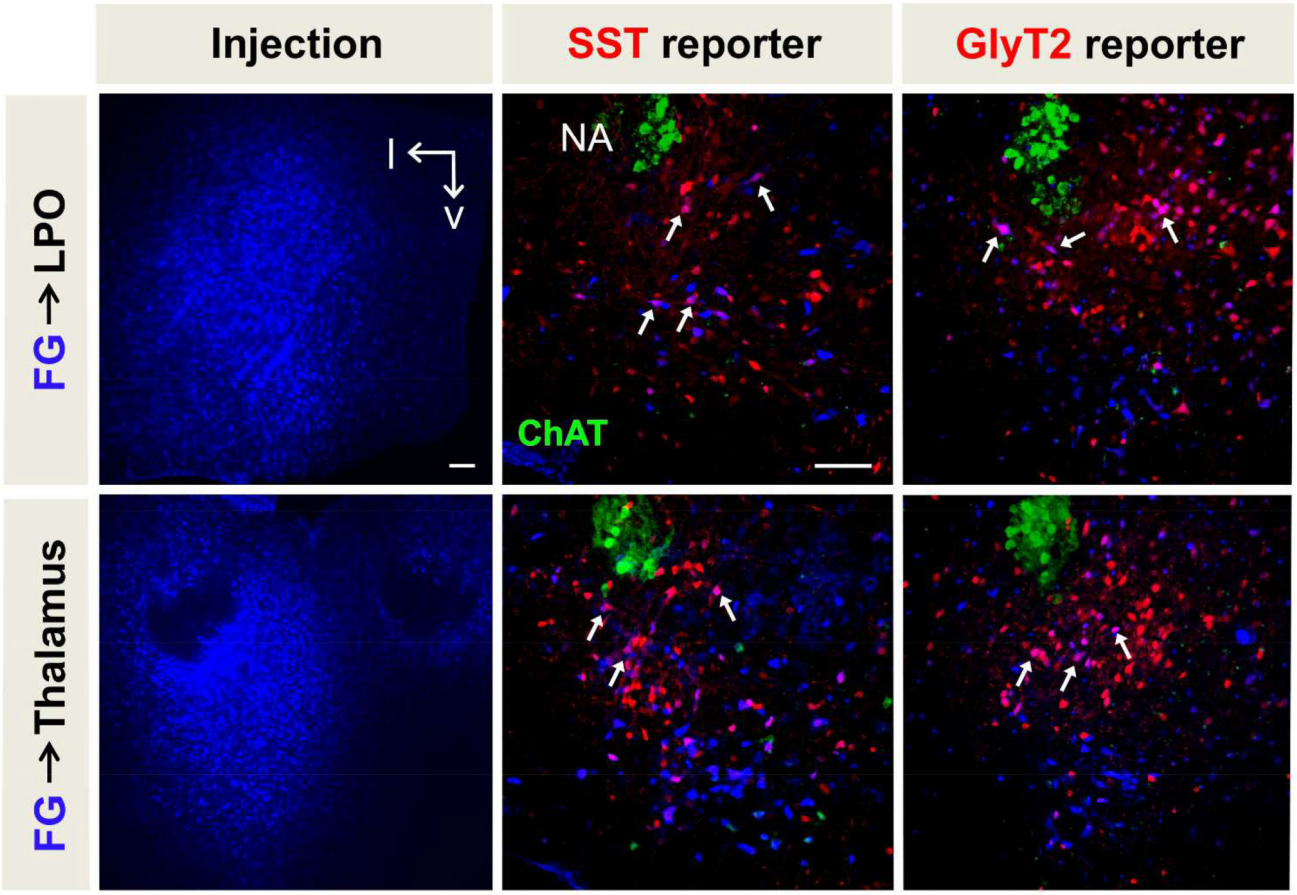

Figure 5.

Retrograde labeling from putative suprapontine target regions. Fluorogold injections into the thalamus (top) and LPO (bottom) result in retrograde labeling of preBötC neurons (white arrows). Injection locations are represented by the blue box in Figs. 3 (thalamus) and 4 (LPO, lateral preoptic area; NA, nucleus ambiguous) Scale bars = 100μm.

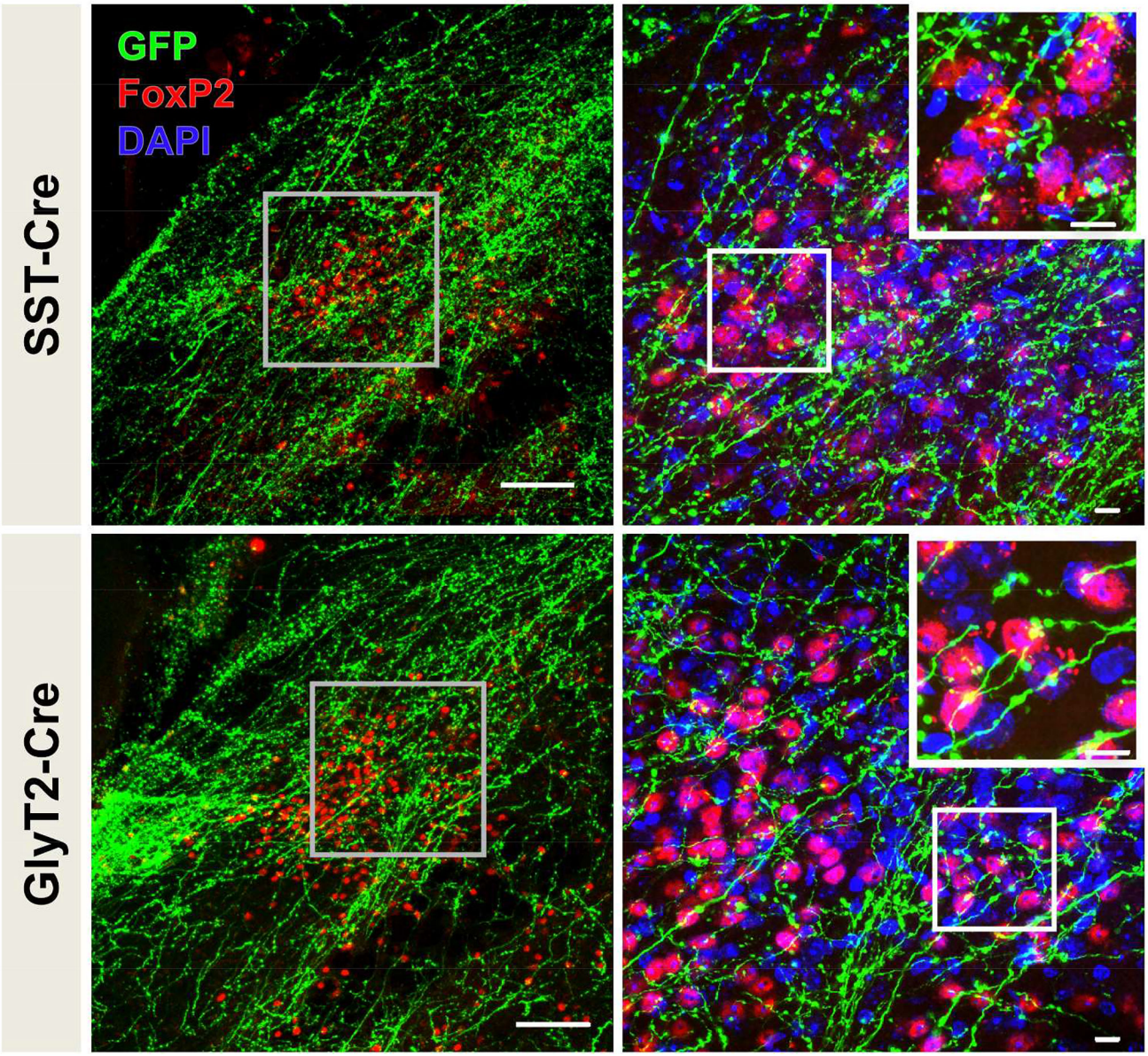

Figure 6.

FoxP2-expressing neurons in the pons receive both SST^+ (top) and $GlyT2^+$ (bottom) preBötC projections. preBötC projections elaborate within the dorsal lateral parabrachial nucleus (left), higher magnification images of boxed regions are shown to the right. More than half of $FoxP2^+$ neurons in the dorsal lateral parabrachial nucleus have puncta from SST + or GlyT2+ preBötC projections directly abutting the cell body (insets to the right). Left scale bar = 100μm; right scale bars = 10μm.

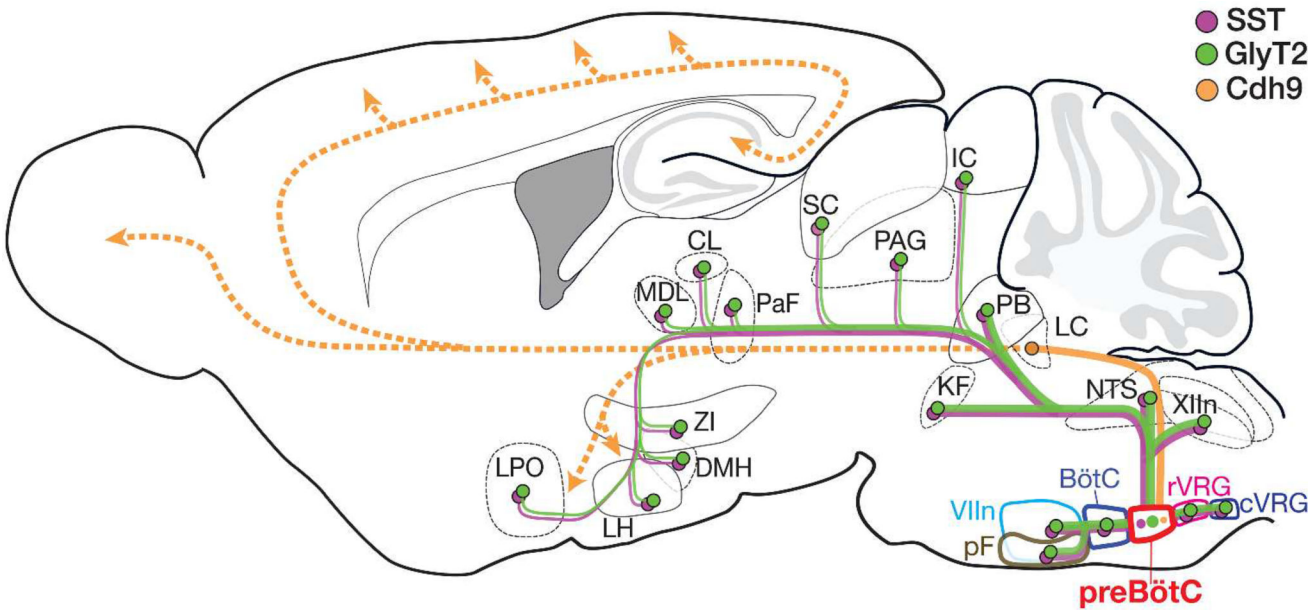

Figure 7.

Summary of the projection profile of SST^+ (purple) and $GlyT2^+$ (green) preBötC neurons. These projections may relay breathing information to higher-order brain regions indirectly via secondary efferents, such as via the parabrachial nuclei/KF (not shown), or via other preBötC subpopulations, e.g., $Cdh9^+$ preBötC neurons (yellow). Abbreviations: BötC, Bötzinger complex; CL, central medial thalamus; cVRG, caudal ventral respiratory group; DMH, dorsomedial hypothalamus; IC, inferior colliculus; KF, Kölliker Fuse; LC, locus coeruleus; LH, lateral hypothalamus; LPO, lateral preoptic area; MDL, medial dorsal thalamus; NTS, nucleus of the solitary tract; PaF, parafascicular thalamus; PAG, periaqueductal gray; PB, parabrachial nuclei; pF, parafacial nucleus; rVRG, rostral ventral respiratory group; SC, superior colliculus; VIIn, facial nucleus; XIIn, hypoglossal nucleus; ZI, zona incerta.